LASER INTERFEROMETER GRAVITATIONAL WAVE OBSERVATORY
- LIGO -
CALIFORNIA INSTITUTE OF TECHNOLOGY
MASSACHUSETTS INSTITUTE OF TECHNOLOGY

Technical Note	**LIGO-T1800273–v4**	2018/09/19

Seismic Cloaking for LIGO

Kaila Nathaniel
Mentors: Brittany Kamai and Rana X. Adhikari

California Institute of Technology
LIGO Project, MS 18-34
Pasadena, CA 91125
Phone (626) 395-2129
Fax (626) 304-9834
E-mail: info@ligo.caltech.edu

Massachusetts Institute of Technology
LIGO Project, Room NW22-295
Cambridge, MA 02139
Phone (617) 253-4824
Fax (617) 253-7014
E-mail: info@ligo.mit.edu

LIGO Hanford Observatory
Route 10, Mile Marker 2
Richland, WA 99352
Phone (509) 372-8106
Fax (509) 372-8137
E-mail: info@ligo.caltech.edu

LIGO Livingston Observatory
19100 LIGO Lane
Livingston, LA 70754
Phone (225) 686-3100
Fax (225) 686-7189
E-mail: info@ligo.caltech.edu

http://www.ligo.caltech.edu/

Abstract

New developments in metamaterials may offer a potential avenue for reducing seismic noise at low frequencies (< 10 Hz). In this study, we investigate the feasibility of using trees as a seismic metamaterial that could shield the LIGO detectors from seismic activity. This seismic cloak would reflect low frequency surface waves away from the detector, thereby increasing the sensitivity of the detectors. This study models the energy transfer from surface waves as they pass through the bandgap filters designed from trees in different arrangements. The attenuation and reflection will hopefully serve to cloak the LIGO detectors from seismic activity. This work could have future impact on high sensitivity detectors, leading to more detections of merger events.

1 Introduction and Literature Review

The LIGO collaboration's goal is to develop gravitational wave astrophysics through the detection of cosmic gravitational waves. The collaboration has built two detectors, located in Hanford, WA, and Livingston, LA. The detectors are laser interferometers with 4km long arms (Figure 1). A laser enters the system and is split into two parts, each of which go down one of the two arms. The beams are then reflected in a mirror, and are read by a photodiode. If a gravitational wave event occurs, spacetime is slightly altered and the length of the beam arm is changed. That change in length puts the two halves of the laser beam out of phase with each other, and that data can be analyzed to find gravitational wave signals [3].

LIGO was designed to measure a wide range of astrophysical sources, but one of the most anticipated first detections was of binary neutron star mergers. Of the six detections that have occurred so far, only one, GW170817, has been of a NS-NS merger, while the rest have all been binary black hole mergers, upending expectations about BBH abundance in the universe.

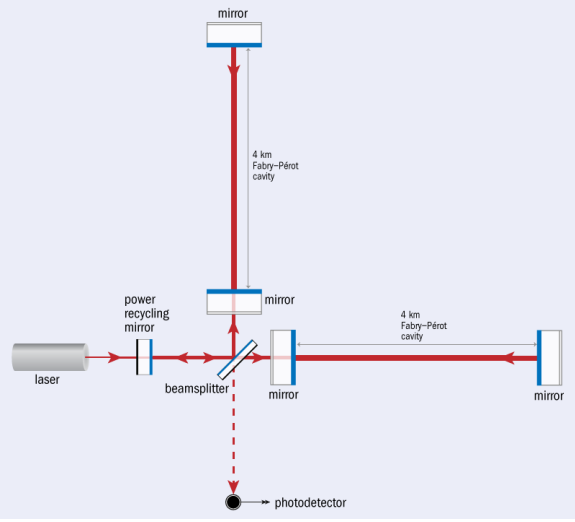

Figure 1: A diagram of the Advanced LIGO detectors [7].

1.1 Limits precision

Ground-based gravitational wave detectors look for signals in the tens to thousands of Hz via laser interferometers, making filtering out astrophysical signals over terrestrial noise difficult. LIGO operates by looking for strain noise,

$$\Delta L = L_1 - L_2 \rightarrow strain = \frac{\Delta L}{L}, \tag{1}$$

where L_1 is the length of the x-arm and L_2 is the length of the y-arm. If there is an increase in strain, then the LIGO team must determine the origin, whether astrophysical or terrestrial. There are many sources of noise in the same band as gravitational wave signals, so reduction of noise is extremely important for data analysis.

Figure 2 describes LIGO's current and past sensitivity. L1 stands for the Livingston, LA detector, and H1 stands for the Hanford, WA detector. Signals below the curves cannot be seen for that configuration. The green trace is from the sensitivity reached using the first generation of the LIGO detectors, Enhanced LIGO. After significant improvements to the technology, Advanced LIGO debuted in 2015. The grey trace is the eventual planned sensitivity after all upgrades are completed. Figure 3 shows the different types of noise that can affect LIGO. The red trace is the measured noise, while the other traces are from predicted and measured noise. There are many different types of noise that limit the precision of the detectors ranging from quantum noise to thermal noise to seismic noise. This study focuses on contributions from seismic and Newtonian noise.

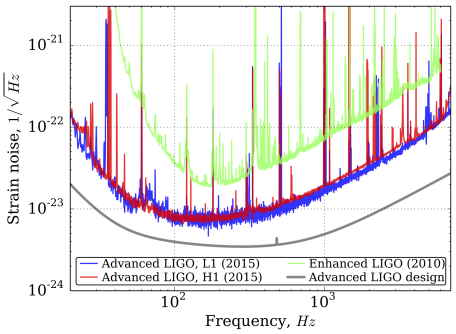

Figure 2: Amplitude spectral density of the detector noise. GW signals that have amplitudes lower than the noise floor cannot be detected with that generation of LIGO [9].

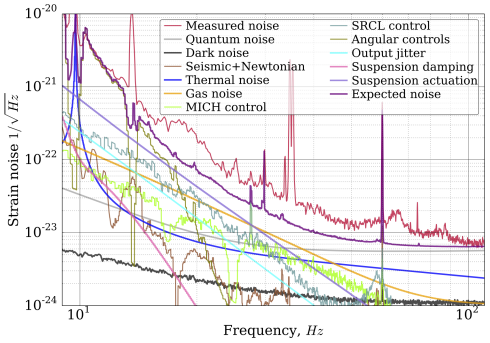

Figure 3: Different types of noise affecting LIGO. The red trace is overall measured noise, while the brown trace is the seismic and Newtonian noise that this paper focuses on [9].

1.2 Seismic noise and LIGO

Seismic noise is a persistent issue for highly precise interferometers, such as gravitational waves. As an example, the gravitational wave strain amplitude of GW170817 (the neutron star merger) was on the order of 10^{-22} [2], while average seismic activity at LIGO-Livingston and LIGO-Hanford is $\sim 10^{-9}$ at 10 Hz [9]. The sensitivity needed to detect such events

necessitates extraordinary noise reduction. Seismic waves affect the differential length measurement by slightly shaking the mirrors.

The LIGO detectors already have significant protection from seismic noise by hanging the test masses from a quadruple pendulum system. The quadruple pendulum system has a resonance as low as 0.4 Hz and isolate up to $1/f^8$ in the detection bandwidth. The pendulums themselves are mounted onto active platforms to provide further isolation. The existing isolation systems work mainly in the 1 Hz to 10 Hz band [9].

1.3 Newtonian noise

Newtonian noise is caused by mass-density fluctuations due to micro-seismic noise, such as from transportation, ocean waves, and construction [4]. As Rayleigh waves move through the ground, they create areas of greater and lesser density in the soil. The fluctuations in mass-density then create small gravitational fields, which can then cause instrument components to shift slightly, thereby shortening or lengthening the beam path.

1.4 Seismic cloaking

One idea to provide further isolation against Newtonian noise is seismic cloaking. Seismic cloaking grew out of the concept of invisibility cloaks, which manipulate electromagnetic waves around an object–making it appear invisible. Shortly after thermodynamic, acoustic and seismic cloaking were investigated. All cloaking is done with metamaterials, which are carefully designed building blocks densely packed into a structure. The structure is usually periodic, but not always [8]. While the majority of metamaterials are artificially made, some natural materials can be manipulated into metamaterials via spacing or other techniques [6].

The first experiment to explore seismic metamaterials was conducted by Brûle et al. in 2014. They created a seismic metamaterial by creating a grid of 5 m deep self-stable holes, diameter of 0.32 m and spaced 1.73 m apart and tested it with a 50 Hz source. They found that the elastic energy was 2.3 times larger at the source than it was in the metamaterial, suggesting that the seismic metamaterial has a significant effect on energy dissipation [5].

A subsequent experiment by Columbi et al. tested trees as a seismic metamaterial in a $\sim$ 6000 m^2 forest of mainly pine trees in Grenoble, France. His team found that the longitudinal resonance inside the trees created two highly attenuating regions around 40 Hz and 110 Hz, which can be seen in Figure 4. They also found that the various sizes and random spacing of the trees produced larger band-gaps than for a uniform configuration, because it created multiple overlapping grids. Columbi theorized that cloaking could be achieved for $\leq$ 10 Hz with trees of longitudinal resonant frequency $\leq$ 10 Hz [6].

The METAFORET project, run by Roux et al. and published in January 2018, expanded upon Colombi's work. METAFORET demonstrated that a dense forest of trees can behave as a locally resonant metamaterial for seismic surface waves. METAFORET compared data from a forest and a canola field and took data with geophones and velocimeters. They measured compressional and flexural resonance in trees and found that compressional resonance was the mechanism that provided filtering for waves. METAFORET used both ambient

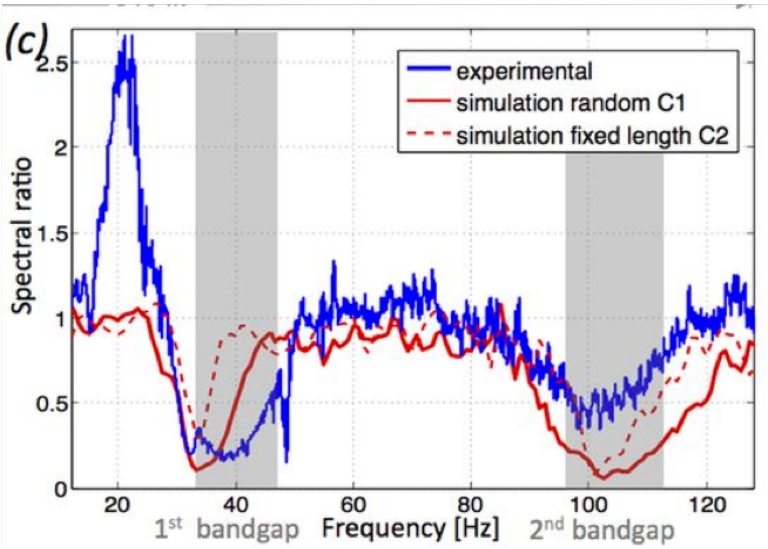

Figure 4: Results from the Colombi et al. 2015 paper [6]. The $x-$axis is the frequency, while the y-axis is spectral ratio, which is the ratio of coherent to incoherent intensity. The blue trace is the experimental results, while the red are simulations. The two gray regions are the attenuating regions both found and predicted.

noise and a 70 kg shaker that excited a 60 s long 10-100 Hz frequency-modulated sweep to determine filtering ability. They found that the cutoff frequency was 50 Hz, and that the most waves were filtered out and cloaked at frequencies between 50 and 80 Hz, as seen in Figure 5 [10]. Roux et al. is currently the most up-to date-work in the field.

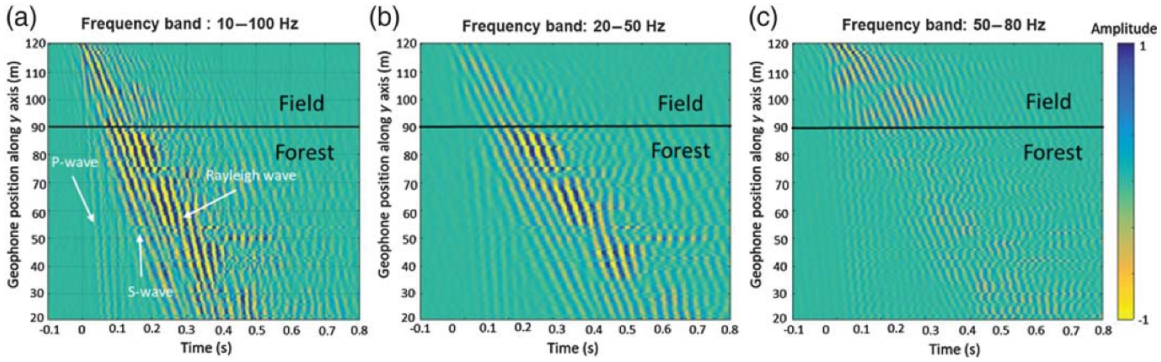

Figure 5: Results from the Roux et al. 2018 paper [10]. Geophone location is plotted against time, with the amplitude of detected waves shown with a colorscale. The plots show that the optimum frequency for this setup is above 50 Hz.

1.5 Seismic cloaking use in LIGO

This study aims to see if the results of Brûle and Columbi can be applied to LIGO. This project will combine theoretical and experimental work by modeling the effects of trees as a way of reducing the noise properties. Further isolating LIGO against seismic noise $\sim$ 50 Hz will further reduce anthropogenic noise. The goal of this study is to determine if

planting trees around the LIGO-Livingston detector will be an effective method of seismic cloaking, and hopefully explore what types of trees or cacti could be used at LIGO-Hanford. Implementing seismic cloaking could both reduce the amplitude of seismic waves, and deflect them away from the detector, thereby enabling better accuracy in signal detection.

1.6 LIGO sensitivity and detection rate

Current estimates place the number of compact binary coalescences per Milky Way Equivalent Galaxy per Myr at around 1000 for a NS-NS merger, 100 for a NS-BH merger, and 30 for a BH-BH merger for realistic estimates. Advanced LIGO is not yet sensitive enough to detect all merger events, so present approximations determine that LIGO can be expected to detect around 40 NS-NS mergers, 10 NS-BH, and 20 BH-BH mergers a year [1]. This is assuming LIGO is constantly observing, so the numbers must be adjusted for the length of observing runs. If seismic cloaking is put into placed at LIGO Livingston or LIGO Hanford, the sensitivity of LIGO would increase, thereby increasing the detection rates.

2 Methods

Much of this project depends on verifying the results of the Columbi paper (2015). Columbi found with experimental and numerical methods that forests could be modeled as locally vertically resonant metamaterials.

2.1 Computational work

2.1.1 Cloaking

Cloaking works by manipulating waves around an object, thereby rendering it invisible to the waves. This is done by creating bandgap filters where the waves are scattered through the cloak and then cancel each other out due to destructive interference [11]. Cloaking has been studied in electromagnetics, acoustics, seismology, and thermodynamics. An object with an electromagnetic cloak is still susceptible to acoustic waves, as different types of cloaks do not work together.

This section studies the energy transfer as waves pass through bandgap filters. It starts by modeling specific aspects of cloaking, then moving into using acoustic cloaking as an analog for seismic cloaking. Acoustic cloaking is similar to seismic cloaking and does not require solving full elastodynamic equations. This is because acoustic and seismic waves have a number of similarities, and can be modeled similarly. Large scale models of acoustic metamaterials could become seismic metamaterials [11].

COMSOL Multiphysics is interactive software designed to simulate physics problems. As seismic cloaking pulls from a number of different fields, models were first created that tested only a single aspect of cloaking. Seismic cloaking requires negative refracting index, as does all electromagnetic, acoustic, and elastodynamic cloaking [8]. As seen in Figure 6, the waves switch direction at the boundary with the negative refracting index. This is the basis of cloaking.

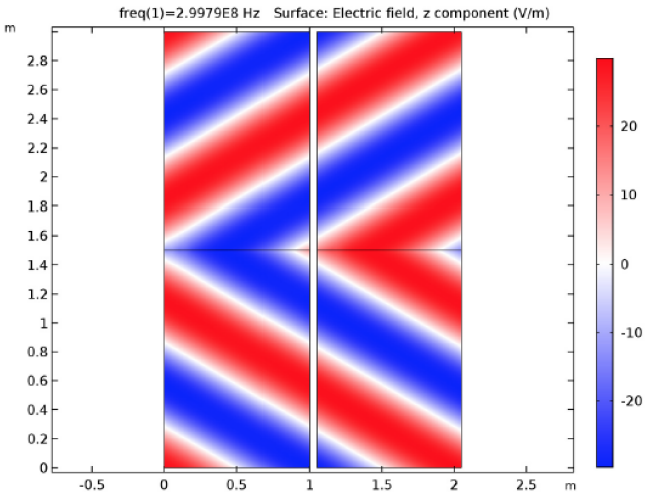

Figure 6: Model of a plane wave traveling through a vacuum (upper) and incident on a metamaterial (lower) with bulk negative permability and permittivity. The block on the left models the wavevector in the material and then adjusts the propagation constant at the boundary for a negative index. The block on the right truncates the domain and acts as an absorbing medium for energy (it is also adjusted for the negative index).

2.1.2 Acoustic cloaking

Starting with acoustic cloaking allows the beginning of quantifying the relationship between the incoming waves and the structure of the cloak. The acoustic cloaking model was initially run with $f = 50, 100, 200, 250, 400$ Hz. The cloak is the most effective at low frequencies, as seen in the comparison between Figure 7 and Figure 11. Interestingly, the cloak mostly evens out the pressure wave to ~ 1.0 Pa at all frequencies, although you can see the beginnings of fluctuations in Figure 9, and it's the most prominent in Figure 11. Oddly, there is a buildup of pressure in the cloak on the right side, which will require further work to determine the cause.

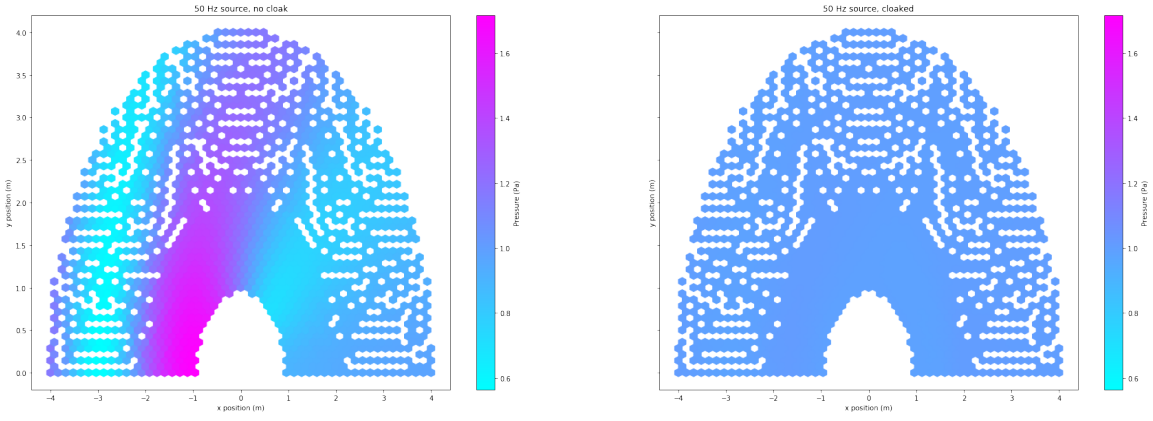

Figure 7: A model of a half circle with and without a cloak. The left image is without a cloak, while the right has a 1 m radius cloak in the inner radius. The incoming wave is at 50 Hz.

All the models were run with the wave propagating in the $+x$ direction. The cloak is made

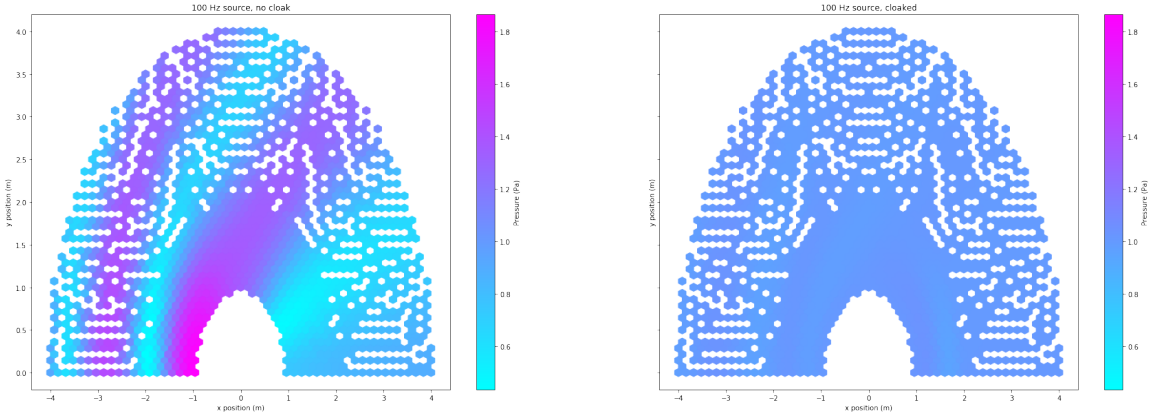

Figure 8: A model of a half circle with and without a cloak. The left image is without a cloak, while the right has a 1 m radius cloak in the inner radius. The incoming wave is at 100 Hz.

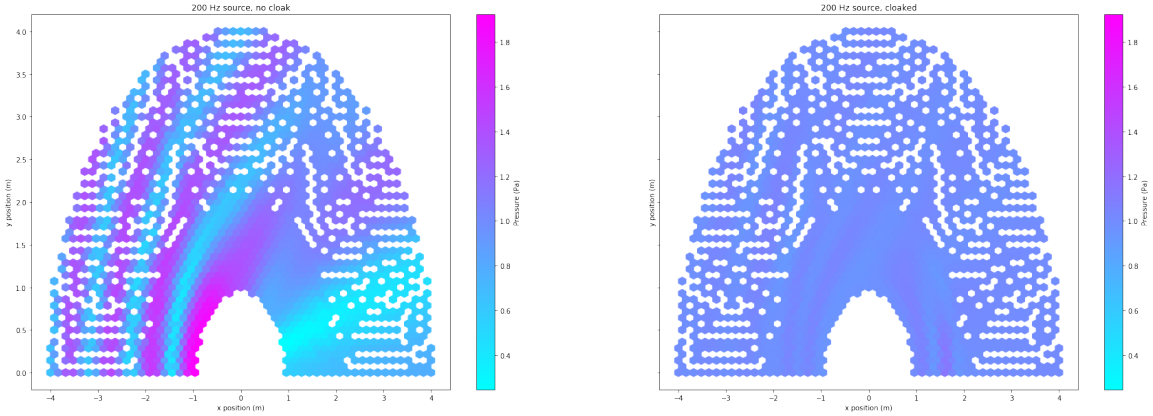

Figure 9: A model of a half circle with and without a cloak. The left image is without a cloak, while the right has a 1 m radius cloak in the inner radius. The incoming wave is at 200 Hz.

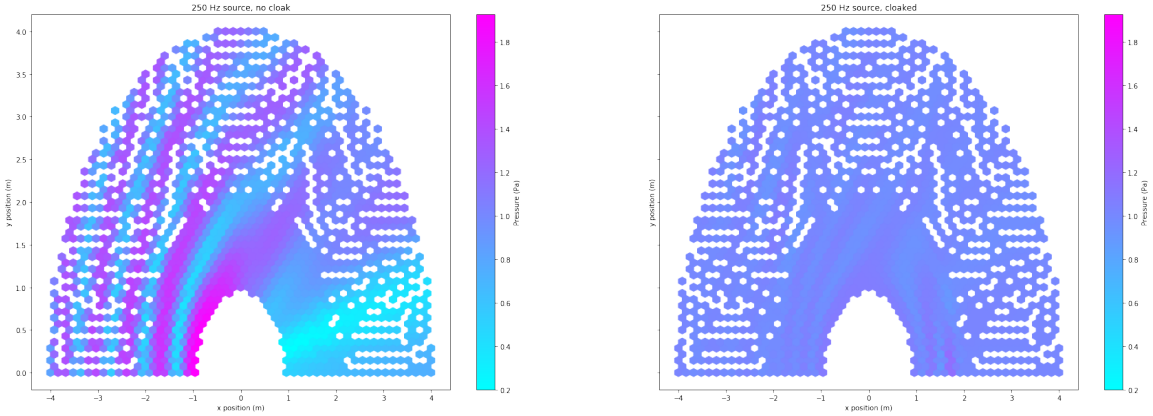

Figure 10: A model of a half circle with and without a cloak. The left image is without a cloak, while the right has a 1 m radius cloak in the inner radius. The incoming wave is at 250 Hz.

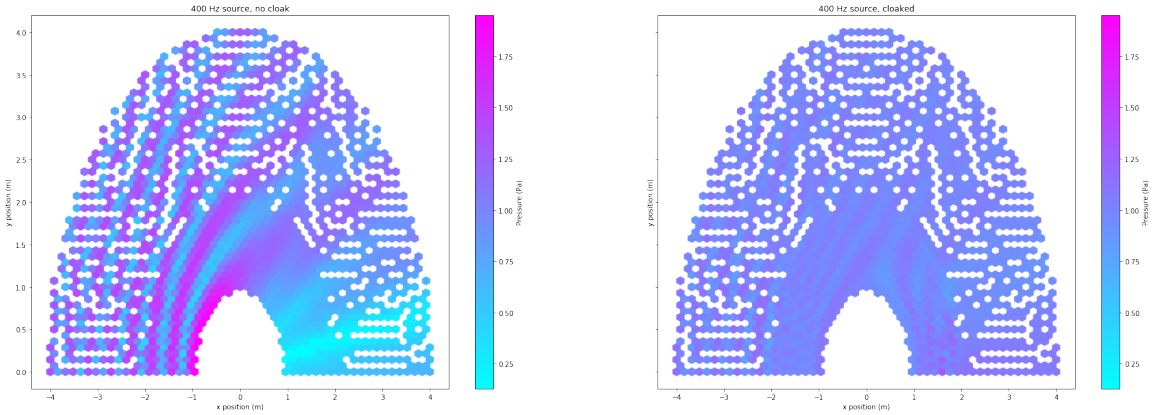

Figure 11: A model of a half circle with and without a cloak. The left image is without a cloak, while the right has a 1 m radius cloak in the inner radius. The incoming wave is at 400 Hz.

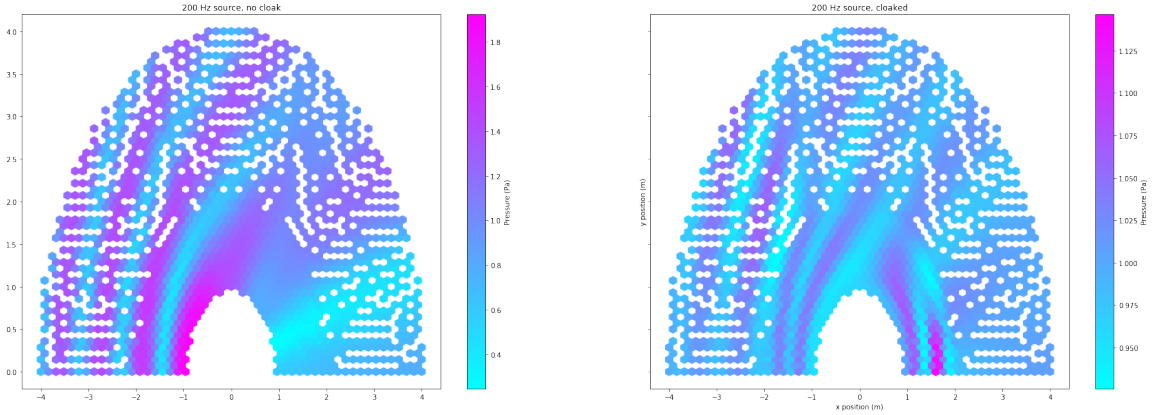

Figure 12: A version of Figure 9 with higher resolution. The left image is without a cloak, while the right has a 1 m radius cloak in the inner radius. The incoming wave is at 200 Hz.

up of 50 layers each 0.02 m thick. The plots show the absolute pressure field, and are plotted with hexagonal binning. The pressure scales for each frequency (the color bar) are identical, although the scale is not identical across the different frequencies. The minimum and maximum for the color bar is set from the minimum and maximum pressure values across both plots for each frequency.

Another view of the model can be seen in Figure 13, which plots the x position against the pressure. You can see the pressure fluctuations on the left half of the plot, like in Figure 12. The uncloaked maroon trace has a large spike against the left boundary of the model, while the cloaked orange version is flat, with only the odd pressure bump on the right side, around $x = 1.5$.

Plots were also made for $f = 100$ and 400 Hz, which can be seen in Figure 14 and Figure 15. It is clear that the 400 Hz model does not work nearly as well as the 200 Hz, model, but it appears that the 100 Hz model actually works better than the 200 Hz. This was unexpected, given that the model was originally designed for 200 Hz.

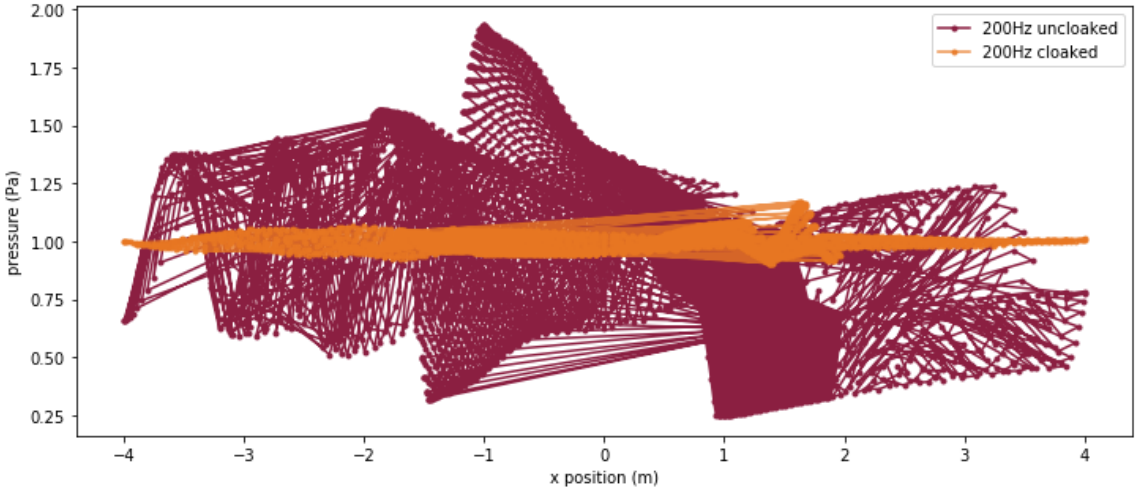

Figure 13: A plot of the x position against the pressure for the half circle model. The frequency is 200 Hz. The maroon trace is the uncloaked model and the orange trace is the cloaked model.

Models were then run with a number of different frequencies large and small, including several that were not integer multiples of the original 200 Hz. The variance in pressure was calculated to see how well the cloak filtered the pressure wave seen in Figure 13. The incoming pressure for the uncloaked model is about the same between 100 Hz and 300 Hz, but starts to change at frequencies below or above. Interestingly, this plot shows that the cloaking effect is about the same for frequencies at 400 Hz and below, but after that the cloak starts rapidly losing effectiveness.

The goal is to be able to get models down to $\leq$ 10 Hz, as that is the noisiest band of seismic noise (see Figure 3), and to lower the floor of the final frequency after the cloak. Effective cloaking at 10 Hz will require redesigning the cloak, as currently the cloaks are not able to hold a full wavelength at 10 Hz, due to the size. Cloaks are able to operate on a subwavelength scale, but at $c_s \approx 400$ m/s, $\nu \approx 40$ m, which is much larger than the $\nu \approx 2$ m found at 200 Hz. Creating a cloak for 10 Hz and below will require a physically larger model,

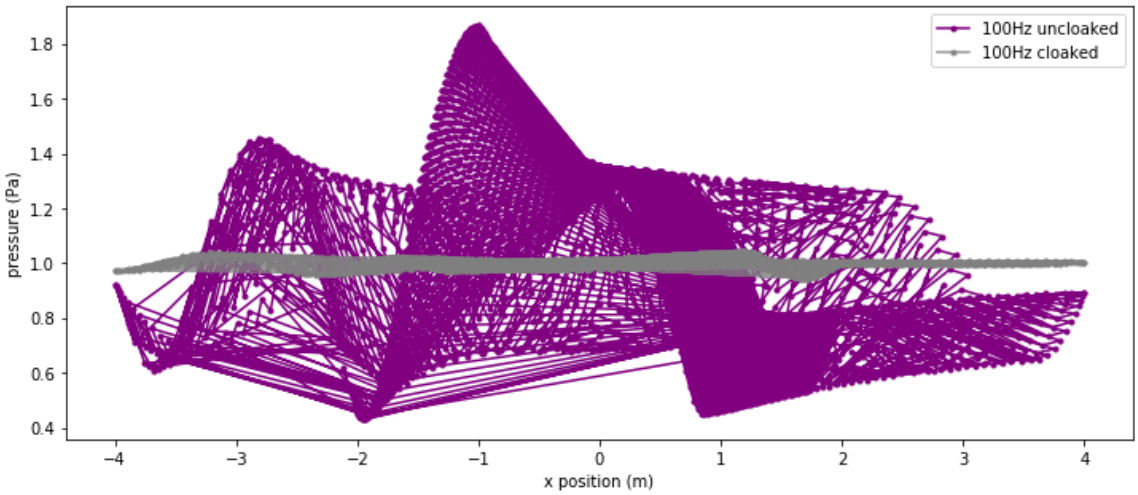

Figure 14: A plot of the x position against the pressure for the half circle model. The frequency is 100 Hz. The purple trace is the uncloaked model and the grey trace is the cloaked model.

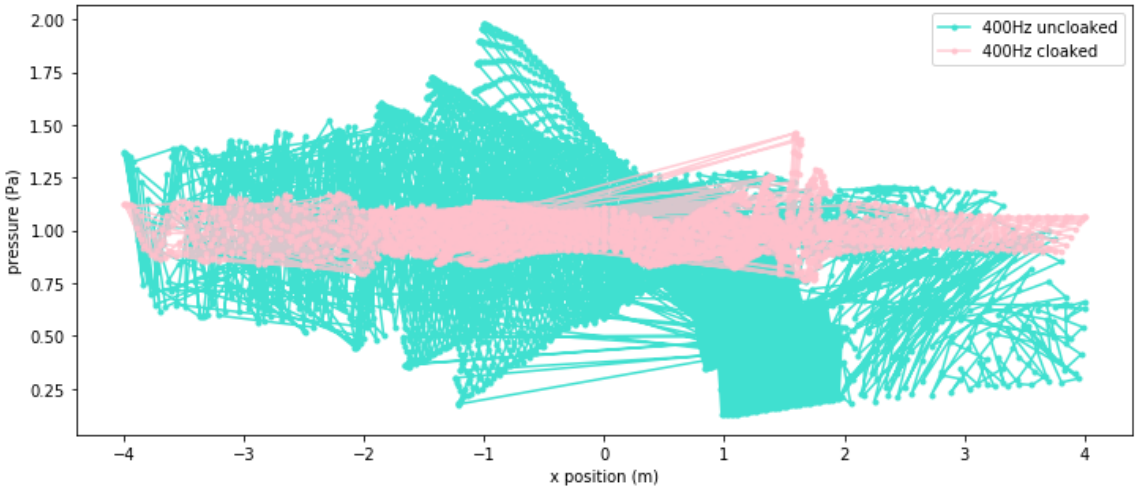

Figure 15: A plot of the x position against the pressure for the half circle model. The frequency is 400 Hz. The turquoise trace is the uncloaked model and the pink trace is the cloaked model.

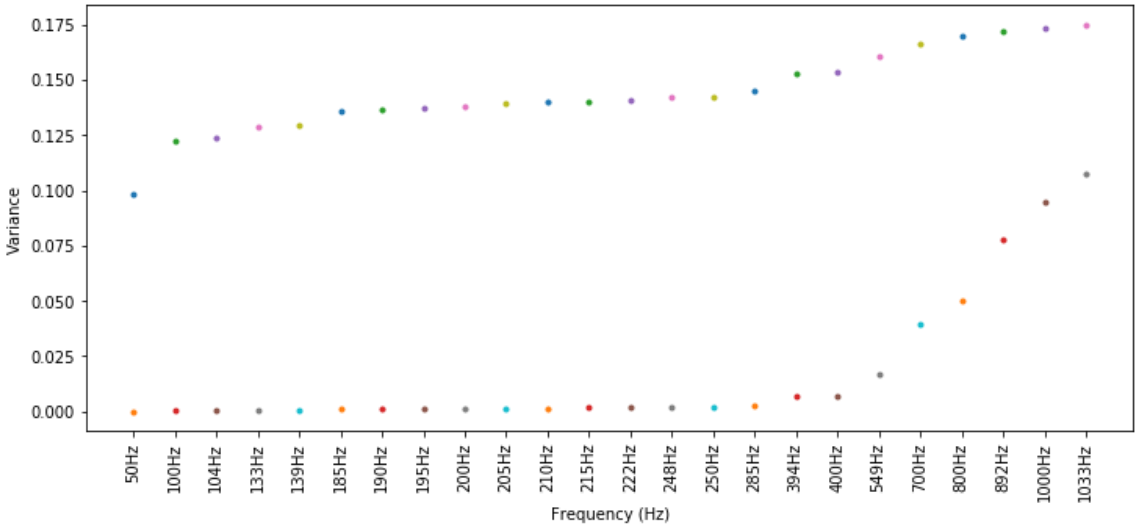

Figure 16: A chart of the different frequencies and the variance in pressure. The top dot is the uncloaked model, and the bottom dot is the cloaked model. The effect of the cloak changes dramatically at frequencies above 400 Hz.

as well as redesigning the cloak. Redesigning the cloak will most likely mean changing the number of layers as well as altering the thickness of the layers.

2.2 Experimental Work

Experimental work was done by taking data at the Los Angeles County Arboretum, which has a variety of plant life and sources of quiet and noise. A birds-eye view of the Arboretum can be seen in Figure 17, with blue dots where we took data. We took data near the freeway, in a quiet grove of trees, and by a waterfall. We used geophones to take data, which use a spring to take a measurement of ground movement and then convert that into a voltage, which can be used to determine the seismic noise.

We set up the geophones and then jumped up and down to ensure that the geophones were picking up data. You can see the data we picked up near the freeway in Figure 18, with the two spikes being jumps. However, you can also see that the data is oscillating around zero, while we were expecting to see a lot of noise from the nearby freeway. The data was then run through a Fast Fourier Transform and compared to a data taken in a quiet grove of trees. If credible data was taken, there should be a large difference between the freeway and trees data. Figure 19 is from 0 to 100 Hz, which is the frequency range we expect for anthropogenic noise, but there is virtually no difference between the freeway and the trees. In fact, in some places the trees data looks noisier than the freeway. This shows that the geophones we used were not sensitive enough for the data we were attempting to collect.

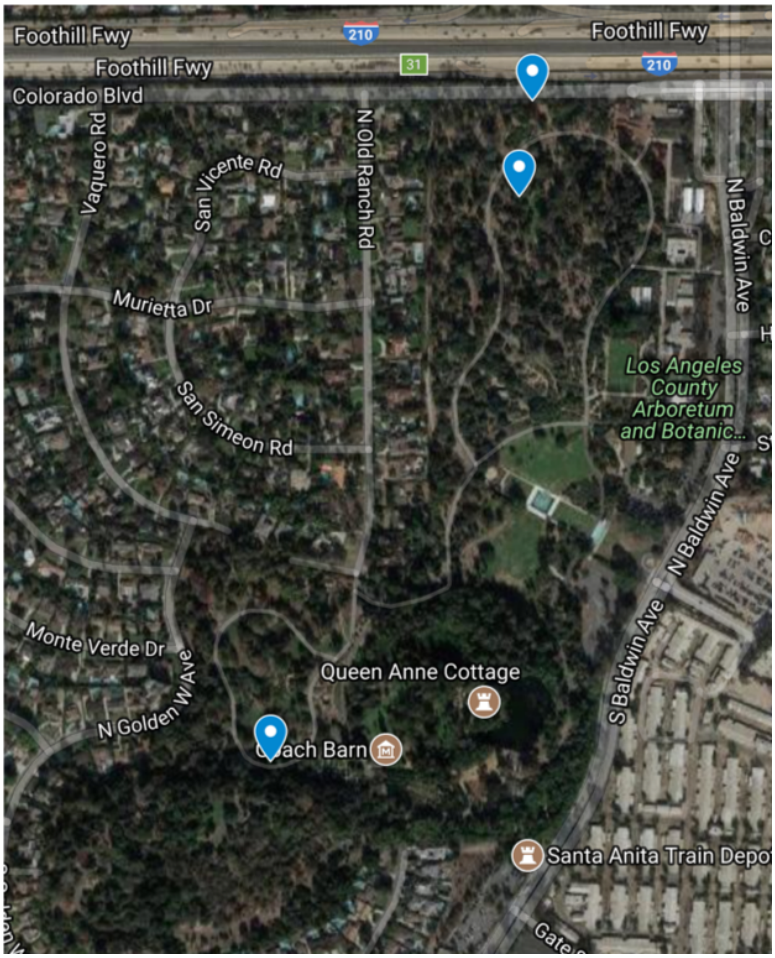

Figure 17: A birds-eye photo of the LA County Arboretum.

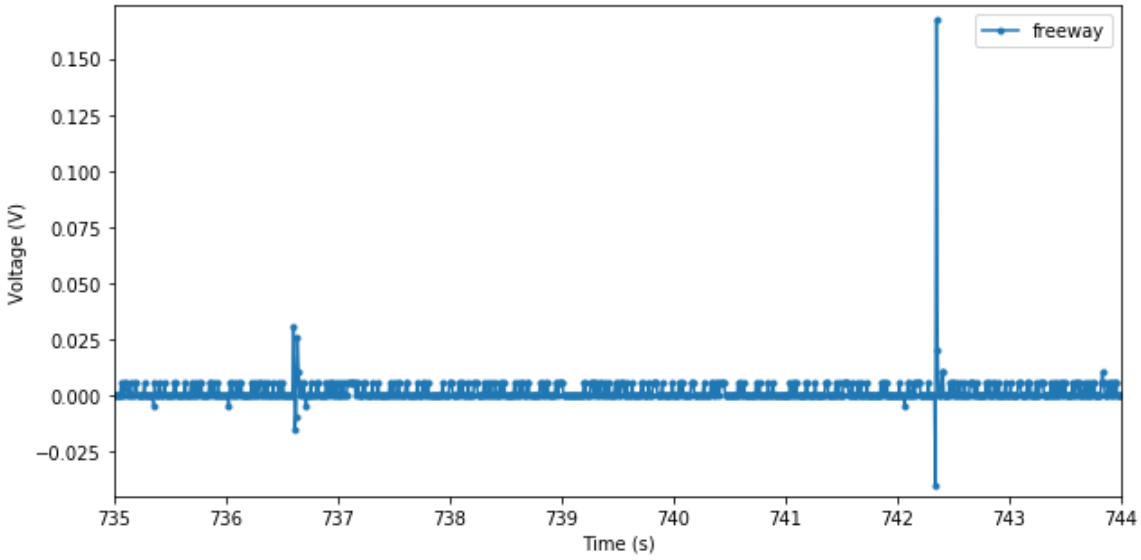

Figure 18: The time plotted against the voltage for the geophone at the freeway. The data is oscillating around zero, except for the calibration spikes.

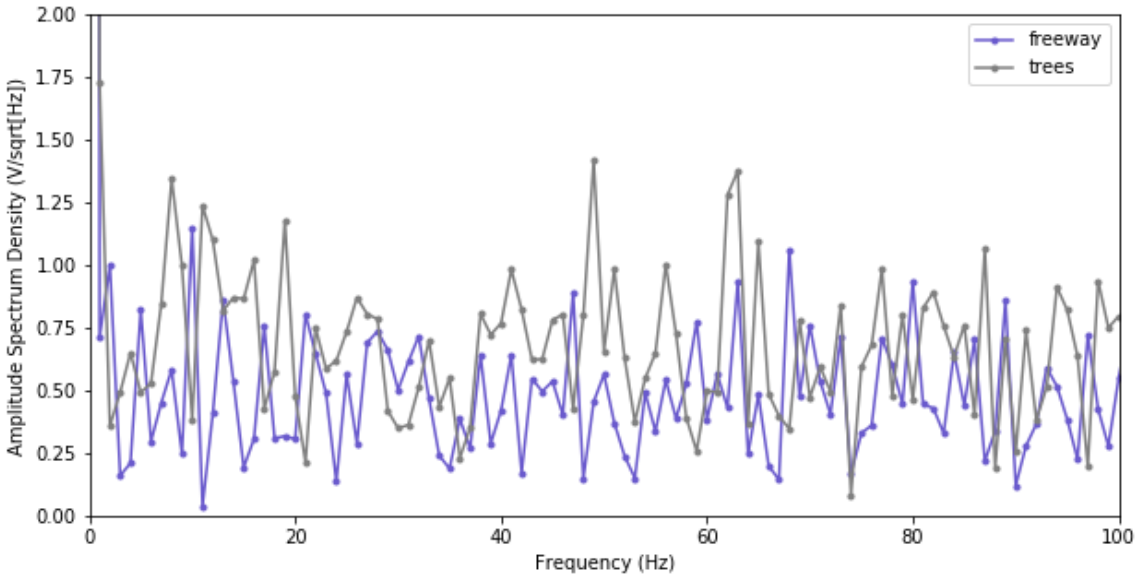

Figure 19: An FFT from 0 to 100 Hz of the freeway and trees data. There is no statistically significant difference in amplitude between the freeway and the trees.

3 Discussion

This project showed that seismic cloaks have a lot of potential, especially for highly sensitive ground-based detectors. Future work needs to involve upgrading models to work for frequencies of 10 Hz and below. We also need to create an actual seismic cloak model, as the models used in this paper were for acoustic cloaking. Extending the experimental work can determine how existing forests of trees can act as seismic cloaks. If we can determine that a preexisting forest can act as a seismic cloak, it could become a parameter for picking locations for future detectors.

The authors are grateful for the support of the US National Science Foundation's Research Experience for Undergraduates Program, award #1757303.

References

[1] J Abadie et al. "Predictions for the rates of compact binary coalescences observable by ground-based gravitational-wave detectors". In: *Classical and Quantum Gravity* 27.17 (Sept. 2010), p. 173001. ISSN: 0264-9381. DOI: 10.1088/0264-9381/27/17/173001.

[2] B.P. Abbott et al. "GW170817: Observation of Gravitational Waves from a Binary Neutron Star Inspiral". In: *Physical Review Letters* 119.16 (Oct. 2017), p. 161101. DOI: 10.1103/PhysRevLett.119.161101.

[3] *About — LIGO Lab — Caltech*. URL: https://www.ligo.caltech.edu/page/about (visited on 06/14/2018).

[4] M Beccaria et al. "Relevance of Newtonian seismic noise for the VIRGO interferometer sensitivity". In: *Class. Quantum Grav* 15.98 (1998), pp. 3339–3362.

[5] S. Brûlé et al. “Experiments on Seismic Metamaterials: Molding Surface Waves”. In: *Physical Review Letters* 112.13 (Mar. 2014), p. 133901. ISSN: 0031-9007. DOI: 10.1103/PhysRevLett.112.133901.

[6] Andrea Colombi et al. “Forests as a natural seismic metamaterial: Rayleigh wave bandgaps induced by local resonances”. In: *Scientific reports* 6 (2016), p. 19238.

[7] IOP Publishing. *LIGO detects first ever gravitational waves - from two merging black holes*. 2016. URL: https://physicsworld.com/a/ligo-detects-first-ever-gravitational-waves-from-two-merging-black-holes/ (visited on 06/27/2018).

[8] Muamer Kadic et al. “Metamaterials beyond electromagnetism”. In: *Reports on Progress in Physics* 76.12 (Dec. 2013), p. 126501. DOI: 10.1088/0034-4885/76/12/126501.

[9] D. V. Martynov et al. “The Sensitivity of the Advanced LIGO Detectors at the Beginning of Gravitational Wave Astronomy”. In: (Apr. 2016). DOI: 10.1103/PhysRevD.93.112004. arXiv: 1604.00439.

[10] Philippe Roux et al. “Toward Seismic Metamaterials: The METAFORET Project”. In: *Seismological Research Letters* 89.2A (Mar. 2018), pp. 582–593. ISSN: 0895-0695. DOI: 10.1785/0220170196.

[11] Ping Sheng. “A Step Towards a Seismic Cloak”. In: *Physics* 7.112 (Mar. 2014), p. 34. ISSN: 1943-2879. DOI: 10.1103/Physics.7.34.